

Generalizable Prompt Tuning for Vision-Language Models

Qian Zhang

Northwestern Polytechnical University
Xi'an, China

ABSTRACT

Prompt tuning for vision-language models such as CLIP involves optimizing the text prompts used to generate image-text pairs for specific downstream tasks. While hand-crafted or template-based prompts are generally applicable to a wider range of unseen classes, they tend to perform poorly in downstream tasks (i.e., seen classes). Learnable soft prompts, on the other hand, often perform well in downstream tasks but lack generalizability. Additionally, prior research has predominantly concentrated on the textual modality, with very few studies attempting to explore the prompt's generalization potential from the visual modality. Keeping these limitations in mind, we investigate how to prompt tuning to obtain both a competitive downstream performance and generalization. The study shows that by treating soft and hand-crafted prompts as dual views of the textual modality, and maximizing their mutual information, we can better ensemble task-specific and general semantic information. Moreover, to generate more expressive prompts, the study introduces a class-wise augmentation from the visual modality, resulting in significant robustness to a wider range of unseen classes. Extensive evaluations on several benchmarks report that the proposed approach achieves competitive results in terms of both task-specific performance and general abilities.

KEYWORDS

Visual-Language Models, Prompt Tuning, Generalization.

1 INTRODUCTION

Over the last decade, deep learning-based models for visual recognition, like VGG [52], ResNet [16], and ViT [10], have made significant progress. These models are typically trained on a large dataset of image and discrete label pairs, where the label is a simple scalar generated by converting a detailed textual description to reduce the computational burden of the loss function. However, this paradigm has two major limitations: (1) the rich semantic relations between textual descriptions are not fully utilized, and (2) the models are limited to closed-set classes only. In recent years, research on large-scale Vision-Language Models (VLMs), such as Contrastive Language-Image Pretraining (CLIP) [47], Flamingo [1], and ALIGN [31], have shown remarkable performance in zero-shot image recognition, indicating potentials for learning open-world visual concepts with this paradigm.

Permission to make digital or hard copies of all or part of this work for personal or classroom use is granted without fee provided that copies are not made or distributed for profit or commercial advantage and that copies bear this notice and the full citation on the first page. Copyrights for components of this work owned by others than ACM must be honored. Abstracting with credit is permitted. To copy otherwise, or republish, to post on servers or to redistribute to lists, requires prior specific permission and/or a fee. Request permissions from permissions@acm.org.

Conference'17, July 2017, Washington, DC, USA

© 2025 Association for Computing Machinery.

ACM ISBN 978-x-xxxx-xxxx-x/YY/MM...\$15.00

<https://doi.org/10.1145/nnnnnnnn.nnnnnnnn>

Method	K=4			K=16		
	Seen	Unseen	H	Seen	Unseen	H
CLIP[47]	65.13	69.02	66.90	65.13	69.02	66.90
CoOp[69]	72.06	59.69	65.29	77.24	57.40	65.86
Ours	74.77	69.14	71.65	77.60	68.36	72.12

Table 1: CLIP with template-based prompts is applicable to a wider range of Unseen classes, but it performs poorly in downstream tasks. CLIP with soft prompts (CoOp) performs well in downstream tasks but lack generalizability. K denotes the number of shots per classes. We use the abbreviation “H” to refer to the Harmonic Mean of “Seen” and “Unseen”, which serves as a measure of efficacy.

In CLIP, the model is trained to associate images and corresponding texts, such that the representations of the two modalities are close in the joint embedding space [47]. The pre-training process involves generating many such image-text pairs from a large corpus of images and texts. Prompt tuning involves finding the best text prompts to use for generating these pairs. This can involve experimenting with different prompts to see which ones lead to the best performance on specific tasks, such as image classification or captioning [38]. Specifically, prompt tuning can be divided into two categories:

Hand-crafted or template-based prompts. One common approach to prompt tuning is to use human evaluation or templates to adjust the prompts [44, 47]. For example, if the task is to recognize objects in images, prompt tuning could involve generating image-text pairs with prompts that emphasize the object category, such as “a photo of a [CLASS]”. [CLASS] refers to a label like “car”.

Soft prompts. Another approach is to use algorithms or other search techniques to explore the space of possible prompts and find the ones that lead to the best performance [6, 32, 61, 68–70]. In this approach, soft prompts are often utilized, represented by the format “{ $v_1, v_2, \dots, v_M, [\text{CLASS}]$ ””, where v_M denotes the learnable vector and is optimized by downstream tasks.

Although previous researches offer some of the advantages mentioned earlier, it also has several significant drawbacks:

1. **Trade-off.** While hand-crafted or template-based prompts can be applied more broadly to unseen classes, they often result in poor performance in downstream tasks (i.e., seen classes). Conversely, soft prompts tend to perform well in downstream tasks, but their lack of the generalizability stems from overfitting to the prompting seen classes (as referred to Table 1).

2. **Expressiveness.** The expressiveness of the prompt subspace is crucial to performance and generalization. Despite having a prompt subspace that is defined on the prompting classes, it may still be insufficient to generalize to a broader range of unseen classes.

3. Multimodality. Prior research has predominantly focused on the textual modality, with very few studies attempting to explore the prompt's generalization potential from the visual modality.

Our contributions. Taking these key challenges into consideration, we conduct a study on how to learn prompts to achieve both a competitive downstream performance and generalization. We propose, for the first time, a prompt tuning method that not only ensembles task-specific and general semantic information from the textual modality but also explores the class-wise augmentation from the visual modality. The study shows that by treating soft and hand-crafted prompts as dual views of the textual modality, and maximizing their mutual information, we can better ensemble task-specific and general semantic information. Moreover, given that the prompting classes are not sufficiently rich to have an expressive prompt subspace, the study introduces a class-wise augmentation from the visual modality, resulting in significant robustness to a wider range of unseen classes. Through extensive evaluations on base-to-new generalization, domain generalization, and cross-dataset transferability settings, we show that the proposed approach achieves competitive results in terms of both task-specific and general abilities.

2 RELATED WORK

2.1 Vision-Language Models

Recent research has demonstrated the necessity of multimodal learning [11, 21, 23, 26, 28, 29] that vision-language models (VLMs) trained on image-text pairs are more capable than those that rely solely on images. This model has received benefits from the advancements in three specific areas. Firstly, text representation learning using Transformers [56] provides better feature representation abilities. Secondly, large-minibatch contrastive representation learning methods [5, 15] help the network to learn discriminative information. Finally, web-scale training datasets [31, 47], which contain billions of image-text pairs for pretraining (0.4 billion pairs for CLIP [47], 1.8 billion pairs for ALIGN [31]), have been utilized. To accurately annotate image-text pairs at the billion level, unsupervised or weakly supervised learning methods [58] are employed in the raw training dataset. Specifically, ViLT [35] improves the robustness of visual and text embedding by randomly masking words in the text. Additionally, masked autoencoders [14] randomly mask patches of the input image to formulate a capable self-supervised learner. CLIP [47] is the representative VLM, which trains the visual encoder and visual encoder using the contrastive loss based on 400 million image-text pairs obtained from the internet, exhibiting impressive zero-shot ability. Recent studies are devoted to improve the generalization ability of VLMs, hallucination issue [25] and OOD [68]. Our study is based on adapting pre-trained VLMs to downstream applications using CLIP, following prompt tuning methods [42, 61, 68–71].

2.2 Prompt Tuning

With the development of deep learning [20, 22, 24, 27, 37, 40, 73, 74], pre-trained VLMs have demonstrated success in various tasks, such as point cloud understanding [65], dense prediction [48], continual learning [54, 66], and visual understanding [49], among others. Prompt tuning [38] is one of the most promising approaches to

adapting pretrained VLMs to specific tasks. Originally introduced in Large Language Models (LLMs), prompt tuning involves hand-crafted instructions (or examples) for the task input to guide the LLMs to generate the appropriate output [4]. Jiang et al. [33] replaced the hand-crafted prompts with candidate prompts obtained through text mining and paraphrasing, and during the training process, they selected the optimal candidates. The gradient-based approach [51] selected the best tokens from the vocabulary that resulted in the most significant changes in gradients, based on the label likelihood. In VLMs, task-related tokens are applied to infer task-specific textual knowledge through prompt tuning. For example, CLIP [47] uses a hand-crafted template, such as “a photo of a [CLASS]”, to model the text embedding for zero-shot prediction.

However, hand-crafted prompts do not consider task-specific knowledge. To address this issue, CoOp [69] replaced hand-crafted prompts with learnable soft prompts optimized by few-shot labeled samples. But, this led to overfitting of the learnable prompts on trained tasks, which undermined their general (zero-shot) ability. Conditional CoOp (CoCoOp) [68] proposed generating conditional context vectors via an extra network and adding them to learnable prompts to alleviate the class drift problem. Similarly, DenseCLIP [48] introduced context-aware prompts via an extra Transformer module to adapt to dense prediction problems. ProDA [42] proposed learning output embeddings of prompts rather than input embeddings. Knowledge-guided CoOp (KgCoOp) [61] introduced a straightforward method to minimize the Euclidean distance between embeddings of hand-crafted and learnable prompts to consider the trade-off between task-specific and general abilities. Visual prompting [2, 19, 32] has also been shown to be an effective tool for large-scale visual models. However, these methods are limited to the Visual Transformer [10] architecture. Vision-language prompt tuning methods [34, 63] generated visual and text prompts via a few learnable parameters to ensure mutual synergy.

Our work is distinct from others in the following ways.

Of the methods mentioned above, our work is most closely related to CoOp [69], CoCoOp [68], ProGrad [70], and KgCoOp [61]. CoOp serves as the baseline method. Based on it, CoCoOp alleviates the overfitting issue by introducing extra conditional context vectors. Both ProGrad and KgCoOp aim to align learnable specific knowledge (i.e., learnable prompt) with general knowledge (i.e., hand-crafted prompt). ProGrad employs Kullback-Leibler (KL) divergence loss and modulates gradient updating to achieve this alignment, while KgCoOp constrains the euclidean distance between embedding distances of learnable and hand-crafted prompts. However, these two methods use hard loss functions and may not achieve optimal results for both task-specific and general abilities. In addition to the challenge of balancing task-specific and general abilities, there is still untapped potential in exploring the visual modality. Our work sets itself apart from others by meticulously addressing these crucial limitations, leading to superior outcomes in terms of the trade-off between task-specific and general abilities (as referred to Section 4).

2.3 Data Augmentation

There is a substantial amount of literature on data augmentation methods to enhance the generalization ability of neural networks.

Recently, label mixing-based approaches, such as Mixup [64], Cutmix [62], and Saliency-Mixup [55], have been shown to significantly improve the generalization of neural networks. These mixup strategies have been successfully employed in various visual tasks, such as continual learning [72] and long-tailed visual recognition [60]. Despite their success, current vision-language prompt tuning methods have not focused on utilizing image augmentation techniques to enhance generalization ability. Interestingly, previous methods that adopted the same Mixup strategy as ours did not show significant improvements and even performed worse in some metrics, as demonstrated in Table 2. One potential reason for this outcome is that, with only learnable parameters in the text inputs, the uninformative pixels generated by Mixup [64] could mislead existing methods and cause them to learn unexpected feature representations, even noises in the under-parameterized regime [41]. Possible solutions to this problem could involve advanced augmentation strategies [55, 62] that selectively mix informative regions of two classes, or update the visual backbone, which could potentially disturb the pre-trained parameters and cause misalignment between visual and textual information. In this work, we innovatively employ a learnable mutual information estimator to maximize the mutual information of dual views of augmented features, which enables us to balance task-specific and general abilities and effectively leverage the augmented visual modality.

2.4 Knowledge Ensemble

Knowledge distillation and sample replay are commonly used in continual learning [8, 72] to mitigate forgetting and adapt to new knowledge. However, prompt tuning for VLMs differs from continual learning as it assumes that the VLMs have already acquired all the necessary knowledge from the pre-training phase and focus on creating a task-specific query. Furthermore, prompt tuning does not have access to the pre-trained data and does not require memory buffers to be revisited frequently. While previous methods [61, 70] for prompt tuning used hard loss function constraints to ensemble task-specific and general knowledge, these achieved sub-optimal trade-offs (as referred to Section 4). Drawing inspiration from self-supervised representation learning [39] that enforces the network to learn invariant feature representations, we treat the embeddings of learnable and hand-crafted prompts as dual views of the text modality and encourage the network to extract shared semantic information by maximizing mutual information. Our approach softly ensembles task-specific and general information and can also accommodate augmented features.

3 METHODOLOGY

Figure 1 provides an overview of the proposed approach. In this section, we first provide a brief review of prompt-based zero-shot inference and learnable soft prompt tuning for the CLIP [47] model. Next, we discuss the motivations behind our proposed method in detail. Finally, we provide a comprehensive introduction to our proposed approach.

3.1 Preliminaries

Zero-shot Inference. CLIP has a strong zero-shot ability [47, 69] due to being pre-trained on minimizing the distance between visual and textual embedding space. Zero-shot inference using the pre-trained CLIP model aims to infer downstream tasks without fine-tuning the model. For instance, in the classification task, zero-shot inference treats it as an image-text matching problem, where text inputs are obtained by a textual template t^{clip} based on the predicted classes. Formally, given the pre-trained vision encoder $\phi(\cdot)$ and text encoder $\theta(\cdot)$, the text embeddings $\mathbf{W}^{clip} = \{\mathbf{w}_i^{clip}\}_{i=1}^{N_c}$ are generated, where the text embeddings of i -th class are denoted by $\mathbf{w}_i^{clip} = \theta(t_i^{clip})$. N_c represents the total number of classes for the downstream task. Then, image features (\mathbf{f}) are extracted from the input image (\mathbf{x}), and the image-text matching score is measured using cosine similarity $\langle \mathbf{w}_i, \mathbf{f} \rangle$. The prediction probability for the i -th class is obtained in this way:

$$p_{zs}^{clip}(\mathbf{w}_i | \mathbf{x}) = \frac{\exp(\langle \mathbf{w}_i, \mathbf{f} \rangle / \tau)}{\sum_{j=1}^{N_c} \exp(\langle \mathbf{w}_j, \mathbf{f} \rangle / \tau)}, \quad (1)$$

where τ is a temperature scalar [47].

Learnable Prompt Tuning. The use of hand-crafted prompts can reduce the distribution gap between pre-training text inputs, but they often lead to poor performance on specific downstream tasks. To address this issue, Context Optimization (CoOp) [69] utilizes a set of continuous context vectors to generate task-specific textual embeddings in an end-to-end manner. Specifically, CoOp incorporates M context vectors and constructs the prompt as $\mathbf{t}_i = \{\mathbf{v}_1, \mathbf{v}_2, \dots, \mathbf{v}_M, \mathbf{c}_i\}$, where $\mathbf{v} = \{\mathbf{v}_1, \mathbf{v}_2, \dots, \mathbf{v}_M\}$ represents the learnable context vectors and \mathbf{c}_i represents the i -th class token embedding. The learnable prompt is then passed to the text encoder $\theta(\cdot)$. The prediction probability for the i -th class is obtained:

$$p^{coop}(\mathbf{t}_i | \mathbf{x}) = \frac{\exp(\langle \theta(\mathbf{t}_i), \mathbf{f} \rangle / \tau)}{\sum_{j=1}^{N_c} \exp(\langle \theta(\mathbf{t}_j), \mathbf{f} \rangle / \tau)}, \quad (2)$$

Then, the few-shot ground-truth labels (\mathbf{y}) serve as the task-specific knowledge, and CoOp optimizes the learnable context tokens \mathbf{v} via the cross-entropy \mathcal{L}_{ce} as follows:

$$\mathcal{L}_{ce}(\mathbf{v}) = - \sum_{i=1}^{N_c} \mathbf{y}_i \log p^{coop}(\mathbf{t}_i | \mathbf{x}). \quad (3)$$

3.2 Motivations

While CoOp-based methods are effective in adapting pre-trained CLIP to downstream tasks, they may cause biases towards the base classes with few-shot training samples, which in turn, negatively impacts generalization ability. To address this issue, Prompt-aligned Gradient (Prograd) [70] has been proposed, which utilizes zero-shot CLIP predictions as general knowledge to guide the optimization direction. Specifically, Prograd employs Kullback-Leibler (KL) divergence between CoOp's prediction and the zero-shot CLIP prediction:

$$\mathcal{L}_{kl}(\mathbf{v}) = - \sum_{i=1}^{N_c} p_{zs}^{clip}(\mathbf{w}_i | \mathbf{x}) \log \frac{p^{coop}(\mathbf{t}_i | \mathbf{x})}{p_{zs}^{clip}(\mathbf{w}_i | \mathbf{x})}. \quad (4)$$

One straightforward approach employed by Knowledge-guided Context Optimization (KgCoOp) [61] is to minimize the Euclidean

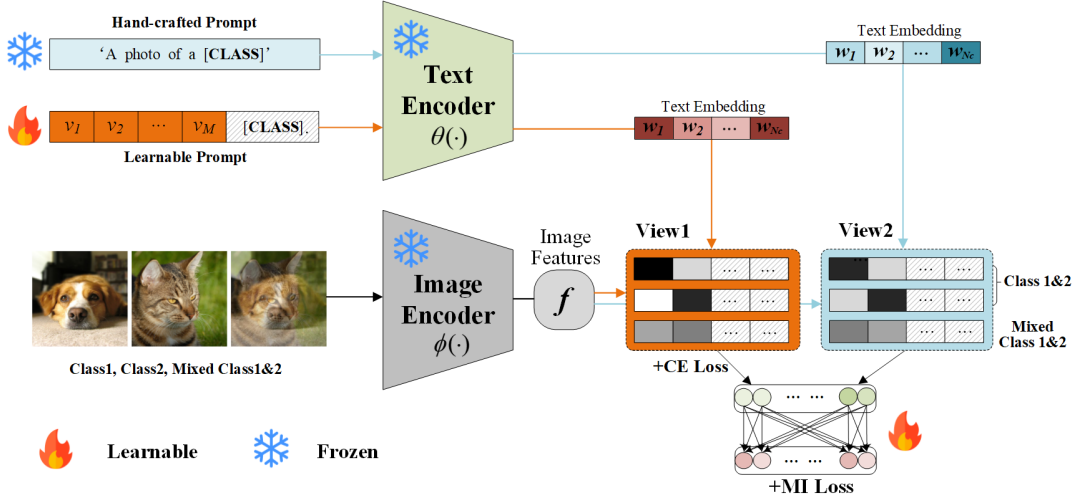


Figure 1: The framework overview. We illustrate our method that is fine-tuned on two classes for the sake of simplicity. We start by fusing the image features from Class 1, Class 2, and Mixed Class 1&2 with the text embeddings of hand-crafted and learnable prompts, respectively. This process allows us to create augmented dual views of the prediction probability. Next, the learnable MI estimator is utilized to ensemble the shared semantic cues from both general and specific information.

distance $\|\cdot\|$ between hand-crafted text embeddings and learnable text embeddings:

$$\mathcal{L}_{kg}(v) = \frac{1}{N_c} \sum_{j=1}^{N_c} \|w_j - \theta(t_j)\|_2^2. \quad (5)$$

Although KgCoOp and ProGrad attempted to address the over-fitting problem, they did not achieve the optimal balance between general and specific information. Specifically, KgCoOp’s use of the Euclidean distance constraint impedes the learnable prompt’s ability to adapt to task-specific information, resulting in weak performance on base classes. For example, in the 16-shot setting, the accuracy of the base class drops by 1.73% compared to CoOp. On the other hand, ProGrad’s use of the KL loss, which is a relatively soft regularization compared to the Euclidean distance, may not fully incorporate the general information from hand-crafted prompts. In the 16-shot setting, the accuracy of new classes is 3.12% lower than KgCoOp (as referred to Section 4).

Furthermore, the existing methods neglect sufficient exploration of image inputs. Conditional CoOp (CoCoOp) [68] addresses this issue by generating a conditional vector for each image with an additional neural network to shift the focus from a specific set of classes to each input sample. However, this conditional design requires an independent forward pass for sample-specific prompts through the text encoder, resulting in significant computation burdens. Additionally, when incorporating hand-crafted general information, we believe that “cross-class information also really matters”, encouraging the network to shift attention to more augmentation classes rather than a fixed set of prompting classes. To overcome these two issues, we propose a novel method and provide detailed explanations below.

3.3 Fusion between Textual Modal Ensemble and Visual Modal Exploration

Textual Modal Ensemble with MI Maximization. To address the first issue discussed earlier, we propose a different approach that treats the hand-crafted and learnable prompts as two complementary views of the text modality, and we maximize the Mutual Information (MI) between them to effectively extract shared semantic information. MI is a fundamental measure of the relationship between random variables [39], and in information theory, the integration of two variables X_1 and X_2 can be achieved by maximizing their MI, as this ensures that the most relevant information is retained:

$$MI(X_1, X_2) = H(X_1) - H(X_1|X_2), \quad (6)$$

where $H(\cdot)$ and $H(\cdot|\cdot)$ represent the information entropy and the conditional entropy. Equivalently, $MI(X_1, X_2)$ can also be reformulated by:

$$MI(X_1, X_2) = MI(X_2, X_1) = H(X_2) - H(X_2|X_1) \\ = H(X_1, X_2) - H(X_1|X_2) - H(X_2|X_1). \quad (7)$$

Given Equations (6) and (7), $MI(X_1, X_2)$ can be reformulated by:

$$MI(X_1, X_2) = \frac{1}{3} [H(X_1) + H(X_2) + H(X_1, X_2)] \\ - \frac{2}{3} [H(X_1|X_2) + H(X_2|X_1)]. \quad (8)$$

The conditional entropy $H(X_1|X_2)$ is expressed as:

$$H(X_1|X_2) = \sum_{x_1 \in X_1, x_2 \in X_2} p(x_1, x_2) \log \frac{p(x_1, x_2)}{p(x_2)}, \quad (9)$$

where $p(x)$ indicates the marginal distributions of x . $p(x_1, x_2)$ represents the joint distribution of x_1 and x_2 . As x_1 and x_2 are dual views of the same set of classes, we force the joint distribution

to be the same as the marginal distributions. $MI(X_1, X_2)$ can be approximated by:

$$MI(X_1, X_2) \approx \frac{1}{3} [H(X_1) + H(X_2) + H(X_1, X_2)]. \quad (10)$$

To estimate the joint probability matrix $P \in \mathbb{R}^{C \times C}$, we follow Invariant Information Clustering [30] to formulate our MI estimator. Given the small batch B_n , the matrix P can be computed by:

$$P = \frac{1}{n} \sum_{i=1}^n \sigma \left[\varphi \left(\mathbf{x}_i^1 \right) \right] \cdot \sigma \left[\varphi \left(\mathbf{x}_i^2 \right) \right]^\top, \quad (11)$$

where \mathbf{x}_i^1 and \mathbf{x}_i^2 are the hand-crafted and learnable embeddings of the same text prompt \mathbf{x}_i , and $\sigma \left[\varphi \left(\mathbf{x}_i^1 \right) \right] = \text{softmax}(z) \in [0, 1]^C$, which can be interpreted as the distribution of a discrete random variable z over C classes, i.e., $P(z = c|x) = \sigma \left[\varphi(x) \right]$. The element in P at the c_1 -th row and c_2 -th column constitutes the joint probability $P_{c_1 c_2} = P(z_1 = c_1, z_2 = c_2)$. The marginal distributions can be obtained by summing over the rows and columns of the matrix P , i.e., $P_{c_1} = P(z_1 = c_1)$, and $P_{c_2} = P(z_2 = c_2)$. As we generally consider symmetric problems and $P_{c_1 c_2} = P_{c_2 c_1}$, P is symmetrized by $P_{c_1 c_2} = \frac{P + P^\top}{2}$. Following [30], we formulate a learnable two-layer Multi-Layer Perceptron (MLP) as the MI estimator to estimate the joint distribution. Moreover, to make the approximate calculation of MI in Equation (8) hold, we apply the distance constraints L_{dc} between the joint distribution and the marginal distributions:

$$\mathcal{L}_{dc}(z_1, z_2) = KL(p(z_1, z_2), p(z_1)) + KL(p(z_1, z_2), p(z_2)), \quad (12)$$

where KL indicates the Kullback-Leibler (KL) divergence loss.

Formally, the total loss function \mathcal{L} is formulated as:

$$\mathcal{L} = \mathcal{L}_{ce}(v) + \lambda_1 \mathcal{L}_{MI}(\mathbf{w}, \theta(t)) + \lambda_2 \mathcal{L}_{dc}(\mathbf{w}, \theta(t)), \quad (13)$$

where \mathbf{w} and $\theta(t)$ represent the embeddings of hand-crafted and learnable prompts, respectively. The first term in Equation (13) aims to optimize the learnable context tokens v like the CoOp-based method in Equation (2). The second and third terms are devoted to ensemble the general and specific information via Mutual Information Maximization (MIM).

Visual Modal Exploration with Class-wise Augmentation.

As mentioned previously, CoCoOp [68] introduced learnable sample-wise information to mitigate the overfitting issue. However, when incorporating hand-crafted general information, we believe that cross-class information is more important. This is due to two reasons: 1) augmented classes encourage the network to pay attention to a broader range of unseen classes rather than just the fixed set of prompting classes, and 2) as Equation (2) shows, the text prompt modulates the image embedding in a class-wise manner. By augmenting the classes, more general cues from hand-crafted prompts are transferred to learnable prompts through MI maximization. To accomplish this, we adopt Mixup [64] for cross-class augmentation. Given two samples x_a and x_b from two classes labeled y_a and y_b ($a \neq b$), Mixup augments x_a and x_b to produce a new training sample x_{ab}^{new} labeled y_{ab}^{new} :

$$\begin{aligned} x_{ab}^{new} &= \lambda x_a + (1 - \lambda) x_b, \\ y_{ab}^{new} &= \lambda y_a + (1 - \lambda) y_b. \end{aligned} \quad (14)$$

where we restrict λ sampling from the interval $[0.4, 0.6]$ to reduce the overlap between the augmented and original classes.

Table 2: We compare the performance of the class-wise augmentation strategy using 4 and 16-shot, and report the average performance across all 11 datasets.

Method	K=4			K=16		
	Base	New	H	Base	Novel	H
CoOp	72.06	59.69	65.29	77.24	57.40	65.86
+ Mixup [64]	71.86	58.72	64.53	76.88	56.72	65.06
Δ	-0.20	-0.97	-0.76	-0.36	-0.68	-0.80
+ SalMix [55]	72.35	61.02	66.13	77.52	58.41	66.41
Δ	+0.29	+1.33	+0.94	+0.28	+1.01	+0.55
ProGrad	73.88	64.95	69.13	77.98	64.41	69.94
+ Mixup [64]	73.15	66.21	68.67	76.44	65.22	69.82
Δ	-0.73	+1.26	+0.46	-1.54	+0.81	-0.12
+ SalMix [55]	74.50	66.91	70.45	77.89	65.62	70.55
Δ	+0.62	+1.96	+1.32	-0.09	+1.21	+0.61
Ours(Mixup)	74.77	69.14	71.65	77.60	68.36	72.12
Ours(w/o Mixup)	74.23	68.23	71.08	77.21	67.43	71.56
Ours(SalMix)	74.97	69.81	71.98	77.92	68.72	72.59

One may ask: “What is the affecting of class-wise augmentation for CoOp-based methods and other approaches that employ hand-crafted general knowledge?” To answer this question, we perform experiments and report the results in Table 2. As KgCoOp [61] only optimizes the text embedding and does not interact with image features, we focus our analysis on CoOp [69] and ProGrad [70]. We find that the Mixup strategy improves the generalization of ProGrad but negatively affects the base classes to some extent. This is because Mixup mixes two samples without discrimination, leading the classifier to learn unexpected feature representations [55, 62], even noises in the under-parameterized regime [41]. ProGrad uses hand-crafted general knowledge to alleviate overfitting but fails in base classes. On the other hand, without hand-crafted general knowledge, CoOp fails in both base and new classes.

To improve the performance of CoOp and ProGrad, we adopt Saliency-based Mixup (SalMix) [55] to mix two samples based on saliency regions and aggregate more appropriate feature representations. We observe significant improvements in the performance of both CoOp and ProGrad, demonstrating the effectiveness of the class-wise augmentation strategy. Unlike CoCoOp [68] and DenseCLIP [48], which require an extra network to induce context-aware prompt, our class-wise augmentation strategy can enrich contextual information in a cost-effective way.

Our proposed method benefits from the mixup strategy in both base and new classes since our learnable MI estimator allows augmented image features to interact effectively with task-specific and general text embeddings to learn informative features. Note that our MI estimator does not add much computation burden (see Section 5.2) and is not used during the inference phase.

4 EXPERIMENT

In accordance with CoCoOp [68], we assess the efficacy of our approach in terms of three aspects: 1. the generalization ability from the base (seen) classes to new (unseen) classes within a dataset [Section 4.1]; 2. domain generalization ability [Section 4.2]; and 3. cross-dataset transferability [Section 4.3]. All our experiments utilize the pre-trained CLIP [47].

Datasets. We evaluate our proposed approach against the first and third aspects, following the settings used in [47, 61, 68–70], and

conduct experiments on 11 datasets: ImageNet[9] and Caltech101 [12] for generic object classification; OxfordPets [46], Flowers102[45], StanfordCars [36], FGVC Aircraft [43], and Food101 [3] for fine-grained classification; UCF101 [53] for action recognition; EuroSAT [17] for satellite image classification; SUN397 [59] for scene classification; DTD [7] for texture classification. For the second aspect, we examine domain generalization by using ImageNet and its variants, with ImageNet serving as the source domain and its variants, including ImageNetV2 [50], ImageNet-Sketch [57], ImageNet-A [13], and ImageNet-R [18], as target domains. Please refer to the Appendix for further information on each dataset.

Training Details. We adopt ResNet-50 [16] as the backbone for the image encoder, with 16 context tokens M , following [69, 70]. The same training epochs, schedule, and data augmentation settings as [69, 70] are used. For all experiments, we set $\lambda_1 = 1$, $\lambda_2 = 2$, and the two-layer MI estimator has hidden dimensions of 256. To ensure fairness, we compute the final performance at least three times with different seeds and average the results. All experiments are carried out on NVIDIA RTX 3090s. For more detailed training settings, please refer to the Appendix.

Baselines. We compare our method with 5 baselines: 1) Zero-shot CLIP [47], which employs the hand-crafted prompts. 2) CoOp [69], which replaces the hand-crafted prompts with a set of learnable prompts trained on the downstream tasks. 3) CoCoOp [68], which improves CoOp by generating the image-conditioned vectors combined with learnable prompts. 4) ProGrad, which optimizes learnable prompts based on hand-crafted gradients. 5) KgCoOp, which regularizes the learnable text embeddings with hand-crafted text embeddings.

4.1 Generalization From Base to New Classes

As in [68, 69], we partition each dataset into two non-overlapping sets of classes: the “base” classes and the “new” classes. To evaluate the generalization ability, all methods are trained on the base classes with a few shot samples for prompt tuning and evaluated on the base and new classes. The class-wise accuracy and Harmonic mean metrics (H, i.e., $HM = \frac{2 \times A_b \times A_n}{A_b + A_n}$) are employed. We conduct experiments on the 1, 2, 4, 8, and 16 shots for comprehensive evaluations. The average performance among all 11 datasets is illustrated in Table 3 and the detailed performance on all 11 datasets with 4 shots is illustrated in Table 4.

Table 3 shows that our method outperforms existing methods in terms of Harmonic mean across all few-shot settings, demonstrating a better trade-off between task-specific and general abilities. Our method also achieves the highest performance on new classes across all settings and the highest performance on base classes for 1, 2, and 4 shot settings. While CoOp-based methods fail to preserve general ability compared to ProGrad and KgCoOp, KgCoOp performs worse than CoOp on base classes with 8 and 16 shots. One possible reason is that the adaptability of the learnable text prompt to the training samples is hindered by the Euclidean distance between the hand-crafted text embeddings and the learnable text embeddings, as shown in Equation (5). In terms of the trade-off between task-specific and general abilities, across all shots settings, KgCoOp surpasses ProGrad on new classes and fails on base classes.

For instance, compared with ProGrad, KgCoOp improves the accuracy on new classes by 3.12% while dropping on base classes by 2.41% for the 16-shot setting. ProGrad slightly exceeds ours on base classes for the 8 and 16-shot settings while obtaining a worse performance on new classes, indicating the generated prompts are serious overfitting on base classes. In summary, our proposed approach demonstrates superior performance across 11 datasets, which confirms that it strikes an optimal balance between adapting task-specific ability to downstream tasks and retaining the general ability of pre-trained VLMs for unseen classes.

Table 4 presents a detailed analysis of the performance of existing methods on 11 datasets. All methods exhibit a significant improvement in the accuracy on base classes compared to zero-shot CLIP. Specifically, CoOp, CoCoOp, ProGrad, and KgCoOp surpass CLIP by 6.84%, 6.68%, 8.86%, and 7.29%, respectively. However, the improved task-specific ability of previous methods results in a bias towards base classes, leading to a significant drop in the general (zero-shot) ability on new classes. As results, previous methods exhibit a drop of 11.40%, 8.93%, 5.30%, and 1.02%, respectively. Our proposed method outperforms prompt tuning methods on new classes as well as zero-shot CLIP, thanks to the class-wise augmentation. We achieve the best accuracy on new classes for 6 out of 11 datasets and the best accuracy on base classes for 8 out of 11 datasets.

4.2 Domain Generalization

Generalizing to out-of-distribution (OOD) data is a crucial skill for machine learning algorithms [67]. As with CoCoOp and ProGrad, we perform prompt tuning on the source dataset (ImageNet [9]) with a few shots and then evaluate the model on the target datasets (ImageNetV2 [50], ImageNet-Sketch [57], ImageNet-A [13], and ImageNet-R [18]). These five datasets have identical classes, but the target datasets have different data distributions from the source dataset.

Table 5 illustrates the results. Our method outperforms all other methods, achieving the best performance on 4 out of 5 datasets, and obtaining the best average accuracy. CoOp and CoCoOp fail in both source and target datasets, indicating that these methods may not fully adapt to downstream tasks and undermine general ability. KgCoOp performs well on OOD datasets but fails on the source dataset, similar to the trend in Section 4.1. ProGrad demonstrates greater domain generalizability than CoOp, CoCoOp, and KgCoOp. Compared to ProGrad, our proposed method achieves a more balanced performance on both source and target datasets.

4.3 Cross-dataset Transferability

We have shown that our approach is generalizable within a dataset. However, transferring to a different dataset can be more challenging since the underlying principles can change completely, such as from object recognition to texture classification. To address this, we follow [68] and tune the text prompt on the source dataset (ImageNet) and evaluate on 10 target datasets. Table 6 shows the performance of compared prompt tuning methods. Our proposed method achieves the best results in 7 out of 11 datasets and has the highest average accuracy. CoOp and CoCoOp are lacking in general knowledge as they are biased to seen classes. ProGrad adapts to

Table 3: Accuracy (%) comparisons among all 11 datasets. K: the number of shots. “Base” and “New”: the classes that are “seen” and “unseen” within a dataset. H: Harmonic mean. The best two results are marked in Bold and Underline (same below).

Methods	K=1			K=2			K=4			K=8			K=16		
	Base	New	H	Base	New	H	Base	New	H	Base	New	H	Base	New	H
CoOp	58.57	53.51	55.92	64.75	52.63	58.07	72.06	59.69	65.29	74.72	58.05	65.34	77.24	57.40	65.86
CoCoOp	64.13	60.42	62.22	67.70	59.36	63.25	71.39	65.74	68.45	73.40	66.42	69.29	75.20	63.64	68.90
ProGrad	68.73	64.98	<u>66.81</u>	<u>71.42</u>	64.00	67.50	73.88	64.95	69.13	76.25	64.74	70.03	77.98	64.41	69.94
KgCoOp	65.79	65.98	65.86	69.67	<u>67.35</u>	<u>68.62</u>	72.42	68.00	70.14	74.08	67.86	70.84	75.51	67.53	71.30
Ours	70.76	68.43	68.61	72.06	69.03	69.70	74.77	69.14	71.65	<u>75.90</u>	68.75	71.61	<u>77.60</u>	68.36	72.12

Table 4: Per-dataset view. Prompts are tuned with 4 shots on base classes.

(a) Average over 11 datasets.				(b) ImageNet.				(c) Caltech101.			
	Base	New	H		Base	New	H		Base	New	H
CLIP	65.13	69.02	66.90	CLIP	64.46	<u>59.99</u>	62.14	CLIP	90.90	90.72	90.81
CoOp	71.97	57.62	62.95	CoOp	64.58	55.81	59.88	CoOp	94.06	87.41	90.61
CoCoOp	71.81	60.09	64.90	CoCoOp	66.28	58.68	62.25	CoCoOp	94.23	86.90	90.42
ProGrad	73.99	63.72	67.91	ProGrad	66.40	58.39	62.14	ProGrad	<u>94.10</u>	89.01	91.48
KgCoOp	72.42	68.00	70.14	KgCoOp	64.78	59.68	<u>62.67</u>	KgCoOp	93.38	<u>91.01</u>	<u>92.18</u>
Ours	74.77	69.14	71.65	Ours	66.80	60.90	63.71	Ours	93.81	92.38	93.08
(d) OxfordPets.				(e) StanfordCars.				(f) Flowers102.			
	Base	New	H		Base	New	H		Base	New	H
CLIP	90.11	94.30	92.16	CLIP	55.55	<u>66.35</u>	60.47	CLIP	68.47	73.90	71.08
CoOp	89.12	91.84	90.46	CoOp	61.54	58.62	60.04	CoOp	88.04	58.23	70.10
CoCoOp	89.46	90.04	89.75	CoCoOp	60.77	54.68	57.56	CoCoOp	87.75	62.08	72.72
ProGrad	<u>91.65</u>	<u>95.13</u>	<u>93.36</u>	ProGrad	64.86	60.77	62.75	ProGrad	<u>89.43</u>	70.28	<u>78.71</u>
KgCoOp	91.50	94.52	92.99	KgCoOp	62.67	66.82	<u>64.68</u>	KgCoOp	85.42	72.04	78.16
Ours	91.87	95.69	93.74	Ours	<u>64.32</u>	64.79	65.53	Ours	90.75	<u>72.27</u>	81.69
(g) Food101.				(h) FGVCIAircraft.				(i) EuroSAT.			
	Base	New	H		Base	New	H		Base	New	H
CLIP	<u>83.71</u>	84.76	84.23	CLIP	19.27	26.45	22.30	CLIP	55.81	66.87	60.84
CoOp	78.03	76.97	77.50	CoOp	20.03	10.82	14.05	CoOp	85.18	33.74	48.33
CoCoOp	78.78	77.43	78.10	CoCoOp	16.69	17.72	17.19	CoCoOp	<u>86.39</u>	50.85	64.02
ProGrad	81.01	81.04	81.02	ProGrad	23.87	20.24	21.91	ProGrad	87.04	44.67	59.04
KgCoOp	82.82	85.15	<u>83.97</u>	KgCoOp	<u>23.95</u>	<u>26.86</u>	<u>25.32</u>	KgCoOp	79.88	57.62	<u>66.75</u>
Ours	83.84	<u>84.81</u>	84.32	Ours	29.28	27.22	28.21	Ours	81.29	<u>61.49</u>	70.02
(j) SUN397.				(k) DTD.				(l) UCF101.			
	Base	New	H		Base	New	H		Base	New	H
CLIP	66.47	70.17	68.27	CLIP	53.12	55.92	54.48	CLIP	68.51	69.77	69.13
CoOp	71.04	61.06	65.67	CoOp	66.71	41.70	51.32	CoOp	73.30	57.62	64.52
CoCoOp	69.86	64.90	67.29	CoCoOp	66.67	41.14	50.88	CoCoOp	73.08	56.52	63.74
ProGrad	<u>73.00</u>	67.83	70.32	ProGrad	<u>67.71</u>	50.40	57.79	ProGrad	<u>74.87</u>	63.17	68.52
KgCoOp	71.82	<u>71.77</u>	<u>71.79</u>	KgCoOp	66.48	<u>55.28</u>	<u>60.36</u>	KgCoOp	73.65	67.57	<u>70.48</u>
Ours	73.12	71.94	72.53	Ours	68.48	56.81	62.1	Ours	77.94	<u>68.32</u>	72.75

Table 5: Quantitative comparisons for the domain generalization, using 4-shot from source.

Method	Source	Target				
	ImageNet	ImageNetV2	ImageNet-Sketch	ImageNet-A	ImageNet-R	Average
CLIP	58.18	51.34	33.32	21.65	56.00	44.10
CoOp	59.51	51.74	30.99	21.23	53.52	43.40
CoCoOp	61.01	53.87	32.65	22.56	54.31	44.88
ProGrad	61.46	54.39	32.86	22.33	55.16	45.44
KgCoOp	59.84	54.02	33.28	22.15	56.24	45.11
Ours	61.53	<u>54.36</u>	35.14	23.01	58.28	46.46

the source dataset but does not perform well in the target datasets. KgCoOp has the excellent general ability and achieves the best results in StandfordCars, Flowers102, and Food 101 datasets while

failing in the source dataset, which is consistent with the previous experiments.

Table 6: Quantitative comparisons for the cross-dataset transferability, using 4-shot from the source.

Method	Source	Target										
	ImageNet	Caltech101	OxfordPets	StanfordCars	Flowers102	Food101	FGVCAircraft	EuroSAT	SUN397	DTD	UCF101	Average
CoOp	61.01	81.58	82.77	48.19	58.91	72.33	9.78	28.93	55.16	30.73	51.56	52.81
CoCoOp	60.43	82.78	83.36	48.86	62.59	74.25	13.82	27.84	57.86	35.82	53.36	54.66
ProGrad	<u>61.46</u>	86.17	85.50	<u>54.26</u>	62.77	74.28	14.13	22.14	56.07	36.47	55.25	55.31
KgCoOp	59.84	<u>87.55</u>	<u>84.93</u>	55.08	64.15	76.57	<u>14.36</u>	25.99	<u>60.28</u>	<u>36.80</u>	<u>58.22</u>	<u>56.69</u>
Ours	61.53	89.01	83.81	53.79	<u>62.87</u>	<u>75.80</u>	15.66	30.22	60.77	39.48	59.21	57.47

Table 7: Ablation studies. “Baseline” refers to the model that only includes the learnable prompt (degrades to CoOp). “MI loss” denotes utilizing Equation (13) to optimize the network. “Aug” denotes class-wise augmentation strategy.

Method	K=4			K=16		
	Base	New	H	Base	Novel	H
Baseline	72.06	59.69	65.29	77.24	57.40	65.86
ProGrad	73.88	64.95	69.13	77.98	64.41	69.94
KgCoOp	<u>72.42</u>	68.00	70.14	<u>75.51</u>	67.53	71.30
+MI loss	74.23	68.23	71.08	77.21	67.43	71.56
+MI loss+Aug	74.77	69.14	71.65	77.60	68.36	72.12

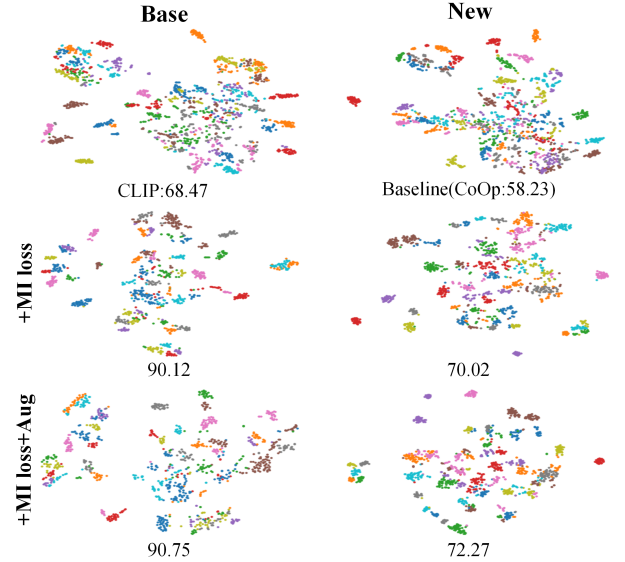
Table 8: Training efficiency comparisons. The *time* indicates the average time to train one image (i.e., ms/image).

	CoOp	CoCoOp	ProGrad	KgCoOp	Ours
<i>time</i>	1.8ms	47ms	6.5ms	1.8ms	4.5ms
H	65.29	68.45	69.13	70.14	71.65

5 ABLATION STUDY

5.1 Effect of Different Components

We evaluate the effectiveness of each component of the proposed method. The results are shown in Table 7. Both ProGrad and KgCoOp introduce general knowledge from hand-crafted prompts and significantly improve performance, particularly in new classes. However, these methods are unable to achieve a desirable trade-off between the base classes and new classes (marked in gray). KgCoOp employs a relatively harder distance constraint (i.e., Euclidean distance) compared to ProGrad, which effectively improves generalization ability but hinders the model’s ability to adapt to specific information. ProGrad modulates the gradient directions but cannot fully utilize general information. Applying MI to ensemble the task-specific and general information achieves a better trade-off between the base classes and new classes by a clear margin. Moreover, the class-wise augmentation from the visual modality enhances the expressiveness of the prompt subspace, resulting in significant robustness to a broader range of new classes. Figure 2 presents t-SNE visualizations of proposed MI loss and the class-wise augmentation strategy, showing that MI loss significantly improves inter-class boundaries and intra-class clustering compared with zero-shot CLIP and CoOp.

**Figure 2: t-SNE visualization on Flowers102 [45].**

5.2 Training Efficiency

Table 8 presents the training time of prompt tuning methods with 4 shots, where the training time is calculated per image (i.e., ms/image). Our proposed method has a significantly lower training time compared to CoCoOp (4.5ms vs 47ms), and it is also faster than ProGrad. CoOp and KgCoOp only optimize the learnable prompt, which takes the least amount of time. It is worth noting that our method does not introduce additional parameters during the inference phase, unlike CoCoOp. The learnable MI estimator in our method is only used during the training phase to facilitate MI estimation and is ablated during the inference phase.

6 CONCLUSION AND FUTURE WORK

In this work, we presented a novel framework as a way of learning generalizable prompts for vision-language models (VLMs) like CLIP, retaining the generalization ability without losing the downstream task performance benefits. We leveraged the hand-crafted prompts and soft prompts as dual views to ensemble semantic information from the textual modality, without introducing extra network modules or laborious operations in the inference phase. Moreover, given that previous studies have mainly concentrated

on the textual modality, we utilized cross-class information to tap into the potential for generalization from the visual modality, an area that has not been extensively explored in previous research. On the other hand, enriching the prompt subspace for VLMs in an unsupervised fashion is still an open area that will help with the usability and expressivity of prompt tuning. Class-wise augmentation provides an effective interface, yet it is unclear what is the optimal way. Here, we presented a simple way of taking enriched prompt subspace via multimodal ensemble and exploration; how to incorporate richer prompt subspace is an interesting direction for future work.

REFERENCES

- [1] Jean-Baptiste Alayrac, Jeff Donahue, Pauline Luc, Antoine Miech, Iain Barr, Yana Hasson, Karel Lenc, Arthur Mensch, Katherine Millican, Malcolm Reynolds, et al. 2022. Flamingo: a visual language model for few-shot learning. *Advances in Neural Information Processing Systems* 35 (2022), 23716–23736.
- [2] Hyojin Bahng, Ali Jahani, Swami Sankaranarayanan, and Phillip Isola. 2022. Exploring Visual Prompts for Adapting Large-Scale Models. *arXiv:2203.17274*
- [3] Lukas Bossard, Matthieu Guillaumin, and Luc Van Gool. 2014. Food-101 – Mining Discriminative Components with Random Forests. In *Computer Vision – ECCV 2014*.
- [4] Tom Brown, Benjamin Mann, Nick Ryder, Melanie Subbiah, Jared D Kaplan, Prafulla Dhariwal, Arvind Neelakantan, Pranav Shyam, Girish Sastry, Amanda Askell, et al. 2020. Language models are few-shot learners. *Advances in neural information processing systems* 33 (2020), 1877–1901.
- [5] Ting Chen, Simon Kornblith, Mohammad Norouzi, and Geoffrey Hinton. 2020. A simple framework for contrastive learning of visual representations. In *International conference on machine learning*. PMLR, 1597–1607.
- [6] Jaemin Cho, Jie Lei, Hao Tan, and Mohit Bansal. 2021. Unifying Vision-and-Language Tasks via Text Generation. In *ICML*, Vol. 139. 1931–1942.
- [7] Mircea Cimpoi, Subhansu Maji, Iasonas Kokkinos, Sammy Mohamed, and Andrea Vedaldi. 2014. Describing Textures in the Wild. In *Proceedings of the IEEE Conference on Computer Vision and Pattern Recognition (CVPR)*.
- [8] Matthias De Lange, Rahaf Aljundi, Marc Masana, Sarah Parisot, Xu Jia, Aleš Leonardis, Gregory Slabaugh, and Tinne Tuytelaars. 2022. A Continual Learning Survey: Defying Forgetting in Classification Tasks. *IEEE Transactions on Pattern Analysis and Machine Intelligence* 44, 7 (2022), 3366–3385.
- [9] Jia Deng, Wei Dong, Richard Socher, Li-Jia Li, Kai Li, and Li Fei-Fei. 2009. ImageNet: A large-scale hierarchical image database. In *2009 IEEE Conference on Computer Vision and Pattern Recognition*. 248–255.
- [10] Alexey Dosovitskiy, Lucas Beyer, Alexander Kolesnikov, Dirk Weissenborn, Xi-aohua Zhai, Thomas Unterthiner, Mostafa Dehghani, Matthias Minderer, Georg Heigold, Sylvain Gelly, Jakob Uszkoreit, and Neil Houlsby. 2021. An Image is Worth 16x16 Words: Transformers for Image Recognition at Scale. *ICLR* (2021).
- [11] Yunfeng Fan, Wenchao Xu, Haozhao Wang, Fushuo Huo, Jinyu Chen, and Song Guo. 2025. Overcome Modal Bias in Multi-modal Federated Learning via Balanced Modality Selection. In *Computer Vision – ECCV 2024*. 178–195.
- [12] Li Fei-Fei, R. Fergus, and P. Perona. 2004. Learning Generative Visual Models from Few Training Examples: An Incremental Bayesian Approach Tested on 101 Object Categories. In *2004 Conference on Computer Vision and Pattern Recognition Workshop*. 178–178.
- [13] Haoran Gao, Hua Zhang, Xingguo Yang, Wenmin Li, Fei Gao, and Qiaoyan Wen. 2022. Generating natural adversarial examples with universal perturbations for text classification. *Neurocomputing* 471 (2022), 175–182.
- [14] Kaiming He, Xinlei Chen, Saining Xie, Yanghao Li, Piotr Dollár, and Ross Girshick. 2022. Masked Autoencoders Are Scalable Vision Learners. In *Proceedings of the IEEE/CVF Conference on Computer Vision and Pattern Recognition (CVPR)*. 16000–16009.
- [15] Kaiming He, Haoqi Fan, Yuxin Wu, Saining Xie, and Ross Girshick. 2020. Momentum Contrast for Unsupervised Visual Representation Learning. In *Proceedings of the IEEE/CVF Conference on Computer Vision and Pattern Recognition (CVPR)*.
- [16] Kaiming He, Xiangyu Zhang, Shaoqing Ren, and Jian Sun. 2016. Deep Residual Learning for Image Recognition. In *Proceedings of the IEEE Conference on Computer Vision and Pattern Recognition (CVPR)*.
- [17] Patrick Helber, Benjamin Bischke, Andreas Dengel, and Damian Borth. 2019. EuroSAT: A Novel Dataset and Deep Learning Benchmark for Land Use and Land Cover Classification. *IEEE Journal of Selected Topics in Applied Earth Observations and Remote Sensing* 12, 7 (2019), 2217–2226.
- [18] Dan Hendrycks, Steven Basart, Norman Mu, Saurav Kadavath, Frank Wang, Evan Dorundo, Rahul Desai, Tyler Zhu, Samyak Parajuli, Mike Guo, Dawn Song, Jacob Steinhardt, and Justin Gilmer. 2021. The Many Faces of Robustness: A Critical Analysis of Out-of-Distribution Generalization. In *Proceedings of the IEEE/CVF International Conference on Computer Vision (ICCV)*. 8340–8349.
- [19] Qidong Huang, Xiaoyi Dong, Dongdong Chen, Weiming Zhang, Feifei Wang, Gang Hua, and Nenghai Yu. 2023. Diversity-Aware Meta Visual Prompting. In *Proceedings of the IEEE/CVF Conference on Computer Vision and Pattern Recognition (CVPR)*.
- [20] Fushuo Huo, Bingheng Li, and Xuegui Zhu. 2021. Efficient wavelet boost learning-based multi-stage progressive refinement network for underwater image enhancement. In *Proceedings of the IEEE/CVF international conference on computer vision*. 1944–1952.
- [21] Fushuo Huo, Ziming Liu, Jingcai Guo, Wenchao Xu, and Song Guo. 2024. UTDNet: A unified triplet decoder network for multimodal salient object detection. *Neural Networks* 170 (2024), 521–534.
- [22] Fushuo Huo, Wenchao Xu, Jingcai Guo, Haozhao Wang, and Yunfeng Fan. 2024. Non-exemplar Online Class-Incremental Continual Learning via Dual-Prototype Self-Augment and Refinement. In *Proceedings of the AAAI Conference on Artificial Intelligence*, Vol. 38. 12698–12707.
- [23] Fushuo Huo, Wenchao Xu, Jingcai Guo, Haozhao Wang, and Song Guo. 2024. C2KD: Bridging the Modality Gap for Cross-Modal Knowledge Distillation. In *Proceedings of the IEEE/CVF Conference on Computer Vision and Pattern Recognition*. 16006–16015.
- [24] Fushuo Huo, Wenchao Xu, Song Guo, Jingcai Guo, Haozhao Wang, Ziming Liu, and Xiaocheng Lu. 2024. ProCC: Progressive Cross-Primitive Compatibility for Open-World Compositional Zero-Shot Learning. *Proceedings of the AAAI Conference on Artificial Intelligence* 38, 11 (Mar. 2024), 12689–12697. <https://doi.org/10.1609/aaai.v38i11.29164>
- [25] Fushuo Huo, Wenchao Xu, Zhong Zhang, Haozhao Wang, Zhicheng Chen, and Peilin Zhao. 2024. Self-Introspective Decoding: Alleviating Hallucinations for Large Vision-Language Models. *arXiv preprint arXiv:2408.02032* (2024).
- [26] Fushuo Huo, Xuegui Zhu, and Bingheng Li. 2022. Three-stream interaction decoder network for RGB-thermal salient object detection. *Knowledge-Based Systems* 258 (2022), 110007.
- [27] Fushuo Huo, Xuegui Zhu, Hongjiang Zeng, Qifeng Liu, and Jian Qiu. 2020. Fast fusion-based dehazing with histogram modification and improved atmospheric illumination prior. *IEEE Sensors Journal* 21, 4 (2020), 5259–5270.
- [28] Fushuo Huo, Xuegui Zhu, Lei Zhang, Qifeng Liu, and Yu Shu. 2021. Efficient context-guided stacked refinement network for RGB-T salient object detection. *IEEE Transactions on Circuits and Systems for Video Technology* 32, 5 (2021), 3111–3124.
- [29] Fushuo Huo, Xuegui Zhu, Qian Zhang, Ziming Liu, and Wenchao Yu. 2022. Real-time one-stream semantic-guided refinement network for RGB-thermal salient object detection. *IEEE Transactions on Instrumentation and Measurement* 71 (2022), 1–12.
- [30] Xu Ji, Joao F. Henriques, and Andrea Vedaldi. 2019. Invariant Information Clustering for Unsupervised Image Classification and Segmentation. In *Proceedings of the IEEE/CVF International Conference on Computer Vision (ICCV)*.
- [31] Chao Jia, Yinfei Yang, Ye Xia, Yi-Ting Chen, Zarana Parekh, Hieu Pham, Quoc Le, Yun-Hsuan Sung, Zhen Li, and Tom Duerig. 2021. Scaling Up Visual and Vision-Language Representation Learning With Noisy Text Supervision. In *ICML*, Vol. 139. 4904–4916.
- [32] Menglin Jia, Luming Tang, Bor-Chun Chen, Claire Cardie, Serge Belongie, Bharath Hariharan, and Ser-Nam Lim. 2022. Visual Prompt Tuning. In *Computer Vision – ECCV 2022*. 709–727.
- [33] Zhengbao Jiang, Frank F. Xu, Jun Araki, and Graham Neubig. 2020. How Can We Know What Language Models Know? *ACL* (2020), 423–438.
- [34] Muhammad Uzair Khattak, Hanoona Rasheed, Muhammad Maaz, Salman Khan, and Fahad Shahbaz Khan. 2023. MaPLE: Multi-modal Prompt Learning. *arXiv:2210.03117*
- [35] Wonjae Kim, Bokyung Son, and Ildoo Kim. 2021. ViLT: Vision-and-Language Transformer Without Convolution or Region Supervision. In *Proceedings of the 38th International Conference on Machine Learning*, Vol. 139. 5583–5594.
- [36] Jonathan Krause, Michael Stark, Jia Deng, and Li Fei-Fei. 2013. 3D Object Representations for Fine-Grained Categorization. In *Proceedings of the IEEE International Conference on Computer Vision (ICCV) Workshops*.
- [37] Bingheng Li and Fushuo Huo. 2024. REQA: Coarse-to-fine assessment of image quality to alleviate the range effect. *Journal of Visual Communication and Image Representation* 98 (2024), 104043.
- [38] Pengfei Liu, Weizhe Yuan, Jinlan Fu, Zhengbao Jiang, Hiroaki Hayashi, and Graham Neubig. 2023. Pre-Train, Prompt, and Predict: A Systematic Survey of Prompting Methods in Natural Language Processing. *ACM Comput. Surv.* 55, 9, Article 195 (jan 2023), 35 pages.
- [39] Xiao Liu, Fanjin Zhang, Zhenyu Hou, Li Mian, Zhaoyu Wang, Jing Zhang, and Jie Tang. 2023. Self-Supervised Learning: Generative or Contrastive. *IEEE Transactions on Knowledge and Data Engineering* 35, 1 (2023), 857–876.
- [40] Ziming Liu, Song Guo, Xiaocheng Lu, Jingcai Guo, Jiawei Zhang, Yue Zeng, and Fushuo Huo. 2023. (ML)\$^2\$SP-Encoder: On Exploration of Channel-Class Correlation for Multi-Label Zero-Shot Learning. In *Proceedings of the IEEE/CVF Conference on Computer Vision and Pattern Recognition (CVPR)*. 23859–23868.

- [41] Zixuan Liu, Ziqiao Wang, Hongyu Guo, and Yongyi Mao. 2023. Over-training with Mixup May Hurt Generalization. In *ICLR*.
- [42] Yuning Lu, Jianzhuang Liu, Yonggang Zhang, Yajing Liu, and Xinmei Tian. 2022. Prompt Distribution Learning. In *Proceedings of the IEEE/CVF Conference on Computer Vision and Pattern Recognition (CVPR)*. 5206–5215.
- [43] Subhransu Maji, Esa Rahtu, Juho Kannala, Matthew B. Blaschko, and Andrea Vedaldi. 2013. Fine-Grained Visual Classification of Aircraft. *CoRR* abs/1306.5151 (2013). <http://arxiv.org/abs/1306.5151>
- [44] Sachit Menon and Carl Vondrick. 2023. Visual Classification via Description from Large Language Models. In *International Conference on Learning Representations*.
- [45] Maria-Elena Nilsback and Andrew Zisserman. 2008. Automated Flower Classification over a Large Number of Classes. In *2008 Sixth Indian Conference on Computer Vision, Graphics & Image Processing*. 722–729.
- [46] Omkar M Parkhi, Andrea Vedaldi, Andrew Zisserman, and C. V. Jawahar. 2012. Cats and dogs. In *2012 IEEE Conference on Computer Vision and Pattern Recognition*. 3498–3505.
- [47] Alec Radford, Jong Wook Kim, Chris Hallacy, Aditya Ramesh, Gabriel Goh, Sandhini Agarwal, Girish Sastry, Amanda Askell, Pamela Mishkin, Jack Clark, Gretchen Krueger, and Ilya Sutskever. 2021. Learning Transferable Visual Models From Natural Language Supervision. In *ICML*, Vol. 139. 8748–8763.
- [48] Yongming Rao, Wenliang Zhao, Guangyi Chen, Yansong Tang, Zheng Zhu, Guan Huang, Jie Zhou, and Jiwen Lu. 2022. DenseCLIP: Language-Guided Dense Prediction With Context-Aware Prompting. In *Proceedings of the IEEE/CVF Conference on Computer Vision and Pattern Recognition (CVPR)*. 18082–18091.
- [49] Hanoona Rasheed, Muhammad Uzair Khattak, Muhammad Maaz, Salman Khan, and Fahad Shahbaz Khan. 2023. Fine-tuned CLIP Models are Efficient Video Learners. In *Proceedings of the IEEE/CVF Conference on Computer Vision and Pattern Recognition (CVPR)*.
- [50] Benjamin Recht, Rebecca Roelofs, Ludwig Schmidt, and Vaishaal Shankar. 2019. Do ImageNet Classifiers Generalize to ImageNet?. In *Proceedings of the 36th International Conference on Machine Learning*, Vol. 97. 5389–5400.
- [51] Taylor Shin, Yasaman Razeghi, Robert L. Logan IV au2, Eric Wallace, and Sameer Singh. 2020. AutoPrompt: Eliciting Knowledge from Language Models with Automatically Generated Prompts. *arXiv:2010.15980*
- [52] Karen Simonyan and Andrew Zisserman. 2014. Very Deep Convolutional Networks for Large-Scale Image Recognition. *CoRR* abs/1409.1556 (2014).
- [53] Khurram Soomro, Amir Roshan Zamir, and Mubarak Shah. 2012. UCF101: A Dataset of 101 Human Actions Classes From Videos in The Wild. *arXiv:1212.0402*
- [54] Vishal Thengane, Salman Khan, Munawar Hayat, and Fahad Khan. 2022. CLIP model is an Efficient Continual Learner. *arXiv:2210.03114*
- [55] A. F. M. Shahab Uddin, Mst. Sirazam Monira, Wheemyung Shin, TaeChoong Chung, and Sung-Ho Bae. 2021. SaliencyMix: A Saliency Guided Data Augmentation Strategy for Better Regularization. *ICLR* (2021).
- [56] Ashish Vaswani, Noam Shazeer, Niki Parmar, Jakob Uszkoreit, Llion Jones, Aidan N Gomez, Łukasz Kaiser, and Illia Polosukhin. 2017. Attention is All you Need. In *Advances in Neural Information Processing Systems*.
- [57] Haoan Wang, Songwei Ge, Zachary Lipton, and Eric P Xing. 2019. Learning Robust Global Representations by Penalizing Local Predictive Power. In *Advances in Neural Information Processing Systems*, Vol. 32.
- [58] Zirui Wang, Jiahui Yu, Adams Wei Yu, Zihang Dai, Yulia Tsvetkov, and Yuan Cao. 2022. SimVLM: Simple Visual Language Model Pretraining with Weak Supervision. *ICLR* (2022).
- [59] Jianxiong Xiao, James Hays, Krista A. Ehinger, Aude Oliva, and Antonio Torralba. 2010. SUN database: Large-scale scene recognition from abbey to zoo. In *2010 IEEE Computer Society Conference on Computer Vision and Pattern Recognition*. 3485–3492.
- [60] Lu Yang, He Jiang, Qing Song, and Jun Guo. 2022. A Survey on Long-Tailed Visual Recognition. *International Journal of Computer Vision* 130 (2022), 1837–1872.
- [61] Hantao Yao, Rui Zhang, and Changsheng Xu. 2023. Visual-Language Prompt Tuning with Knowledge-guided Context Optimization. In *CVPR*.
- [62] Sangdoo Yun, Dongyoon Han, Seong Joon Oh, Sanghyuk Chun, Junsuk Choe, and Youngjoon Yoo. 2019. CutMix: Regularization Strategy to Train Strong Classifiers With Localizable Features. In *Proceedings of the IEEE/CVF International Conference on Computer Vision (ICCV)*.
- [63] Yuhang Zang, Wei Li, Kaiyang Zhou, Chen Huang, and Chen Change Loy. 2022. Unified Vision and Language Prompt Learning. *arXiv:2210.07225*
- [64] Hongyi Zhang, Moustapha Cissé, Yann N. Dauphin, and David Lopez-Paz. 2017. mixup: Beyond Empirical Risk Minimization. *ICLR* (2017).
- [65] Renrui Zhang, Ziyu Guo, Wei Zhang, Kunchang Li, Xupeng Miao, Bin Cui, Yu Qiao, Peng Gao, and Hongsheng Li. 2022. PointCLIP: Point Cloud Understanding by CLIP. In *Proceedings of the IEEE/CVF Conference on Computer Vision and Pattern Recognition (CVPR)*. 8552–8562.
- [66] Zangwei Zheng, Mingyuan Ma, Kai Wang, Ziheng Qin, Xiangyu Yue, and Yang You. 2023. Preventing Zero-Shot Transfer Degradation in Continual Learning of Vision-Language Models. *arXiv:2303.06628*
- [67] Kaiyang Zhou, Ziwei Liu, Yu Qiao, Tao Xiang, and Chen Change Loy. 2023. Domain Generalization: A Survey. *IEEE Transactions on Pattern Analysis and Machine Intelligence* 45, 4 (2023), 4396–4415.
- [68] Kaiyang Zhou, Jingkang Yang, Chen Change Loy, and Ziwei Liu. 2022. Conditional Prompt Learning for Vision-Language Models. In *Proceedings of the IEEE/CVF Conference on Computer Vision and Pattern Recognition (CVPR)*. 16816–16825.
- [69] Kaiyang Zhou, Jingkang Yang, Chen Change Loy, and Ziwei Liu. 2022. Learning to prompt for vision-language models. *International Journal of Computer Vision* 130 (2022), 2337–2348.
- [70] Beier Zhu, Yulei Niu, Yucheng Han, Yue Wu, and Hanwang Zhang. 2022. Prompt-aligned Gradient for Prompt Tuning. *arXiv:2205.14865*
- [71] Beier Zhu, Yulei Niu, Saeil Lee, Minhoe Hur, and Hanwang Zhang. 2023. Debaised Fine-Tuning for Vision-language Models by Prompt Regularization. In *AAAI*.
- [72] Fei Zhu, Zhen Cheng, Xu-yao Zhang, and Cheng-lin Liu. 2021. Class-Incremental Learning via Dual Augmentation. In *Advances in Neural Information Processing Systems*, Vol. 34. 14306–14318.
- [73] Xuegui Zhu, Yu Shu, Chaopeng Luo, Fushuo Huo, and Wang Zhu. 2020. Transient electromagnetic voltage imaging of dense UXO-like targets based on improved mathematical morphology. *IEEE Access* 8 (2020), 150341–150349.
- [74] Xuegui Zhu, Yu Shu, Qian Zhang, and Fushuo Huo. 2022. Spatiotemporal regularization correlation filter with response feedback. *Journal of Electronic Imaging* 31, 4 (2022), 043017–043017.